Journal of
Materials Chemistry B

RSC Publishing

PAPER

View Article Online
View Journal

Cite this: DOI: 10.1039/c3tb20639d

Irreversible evolution of eumelanin redox states detected by an organic electrochemical transistor: en route to bioelectronics and biosensing

Giuseppe Tarabella,*[a] Alessandro Pezzella,*[b] Agostino Romeo,[a] Pasquale D'Angelo,[a] Nicola Coppedè,[a] Marco Calicchio,[a] Marco d'Ischia,[b] Roberto Mosca[a] and Salvatore Iannotta[a]

Received 2nd May 2013
Accepted 5th June 2013

DOI: 10.1039/c3tb20639d

www.rsc.org/MaterialsB

Organic electrochemical transistors (OECTs) are currently emerging as powerful tools for biosensing, bioelectronics and nanomedical applications owing to their ability to operate under liquid phase conditions optimally integrating electronic and biological systems. Herein we disclose the unique potential of OECTs for detecting and investigating the electrical properties of insoluble eumelanin biopolymers. Gate current measurements on fine aqueous suspensions of a synthetic eumelanin sample from 5,6-dihydroxyindole (DHI) revealed a well detectable hysteretic response similar to that of the pure monomer in solution, with the formal concentration of the polymer as low as 10^{-6} M. Induction of the gate current would reflect electron transfer from solid eumelanin to the Pt-electrode sustained by redox active catechol/quinone components of the polymer. A gradual decrease in gate current and areas subtended by hysteretic loops were observed over 5 cycles both in the eumelanin- and DHI-based devices, suggesting evolution of the polymer from a far-from-the-equilibrium redox state toward a more stable electronic arrangement promoted by redox exchange with the gate electrode. OECTs are thus proposed as valuable tools for the efficient heterogeneous-phase sensing of eumelanins and to gauge their peculiar electrical and redox behaviour.

1 Introduction

The dynamic response of human skin and eyes to sun exposure and oxidative stress relies for the most part on the unique physicochemical properties of eumelanins, the black insoluble biopolymers produced by oxidative polymerization of 5,6-dihydroxyindole (DHI) and related metabolites.[1] The central role of eumelanins in skin and eye photoprotection, free radical scavenging and melanoma genesis[2–4] has prompted intense studies across biology, chemistry, and physics to gain insights into the intriguing mechanisms by which damaging UV radiation and reactive oxygen species are efficiently captured and quenched by the biopolymer.[2] Parallel to the rapid advances in the elucidation of the primary structure and supramolecular architecture of natural eumelanins,[3,5] considerable attention has been focused over the past decade on the development of synthetic mimics for technological applications, including surface coating and thin films for organic electronics.[6]

Three peculiar yet highly elusive properties of eumelanins have especially intrigued physicists and materials scientists: their black chromophore, with a broad featureless optical absorption and near unity nonradiative conversion of absorbed photon energy; their paramagnetic character, revealed by a permanent signal in the electron paramagnetic (EPR) spectrum; and their electrical behaviour showing photoconductivity in the solid state.[2] Elucidation of these properties may provide new impetus toward application of eumelanins as soft, biocompatible and bioavailable functional polymers for organoelectronic devices and biointerfaces. Prospects in this field are exemplified by the burst of technological research on polydopamine, a peculiar eumelanin-like biopolymer resembling neuromelanin[7,8] produced by the auto-oxidation of dopamine at alkaline pH, which combines unique adhesion properties[9] with semiconductor-like behaviour.[6,10] Although early observations[11] supported an amorphous semiconductor-like behaviour, more recent studies demonstrated that optical and electrical properties of eumelanins can be better accounted for by alternative models, *e.g.* the chemical disorder model,[12] which takes into account a supposedly high molecular heterogeneity and the lack of a well defined optical gap. These concepts, together with the strong dependence of the electrical and EPR properties on the degree of hydration, support the view that eumelanin behaves like an electronic–ionic hybrid conductor.[13] Electrical

[a]*Institute of Materials for Electronics and Magnetism (IMEM), National Research Council (CNR), Parma, Italy. E-mail: giuseppe.tarabella@imem.cnr.it; Fax: +39 0521 269206; Tel: +39 0521 269294*

[b]*Department of Chemical Science, University of Federico II, Naples, Italy. E-mail: alessandro.pezzella@unina.it; Tel: +39 08 1674130*

conductivity would thus be induced by hydration, which defines the balance of comproportionation/disproportionation equilibria between hydroxyquinone, semiquinone and quinone species so as to dope electrons and protons into the system, opening exciting possibilities for bioelectronic applications such as ion-to-electron transduction.

Despite the increasing recognition of both pro-oxidant and antioxidant behaviours of eumelanins with important medical implications, electrical characterization of these polymers has been carried out for the most part on thin films or bulk solids, since colloidal eumelanin particles have been reported to be typically electrochemically silent.[14]

On this basis, direct investigation of eumelanin electrical response in a more biomimetic aqueous suspension state is a challenging issue in view of the possible development of a biosensor aimed at assessing biopolymer concentration and redox state in its environment. Dysfunctions of eumelanin levels have been associated with different disorders, from melanoma (the most diffuse skin cancer) to neurodegenerative disorders, and the direct determination of eumelanin redox states and levels in a pathological setting would be an ambitious yet highly desirable goal.

Recently, organic electrochemical transistors based on conductive polymers, such as poly(3,4-ethylenedioxythiophene):poly(styrene sulfonate), PEDOT:PSS, have emerged as ideal platforms to interface bio-signalling with electronics.[15,16] These devices appear to be most suited for biosensing, due to their ability to work in liquid environments at low voltages (<1 V). In this respect, several studies dealing with OECTs as sensing devices for different species of analytes, such as hydrogen peroxide,[17,18] glucose[19,20] or ions,[21] have been published. More complex systems, such as DNA, dopamine and cells, have been reported in the literature,[22] together with some emerging developments in neuroscience, consisting of the control of electronic ion signalling in individual cells,[23] monitoring of brain electrical activity[24] and delivery or detection of neurotransmitters.[25,26]

Herein, we disclose an organic electrochemical transistor based on PEDOT:PSS as a biosensor device allowing for the first time detection and characterization of a colloidal suspension of a synthetic eumelanin from DHI. With detection sensitivity up to 10^{-6} M formal concentration, the OECT is the first purposeful device to detect insoluble redox-active materials and to provide insights into their electrical behaviour in aqueous suspensions by analysis of the gate current.

2 Experimental

2.1 Device fabrication and characteristics

A solution of poly(3,4-ethylenedioxythiophene):poly(styrene sulfonate), PEDOT:PSS (Clevios PH500, purchased from Heraeus Conductive Polymers Division), has been doped with ethylene glycol 20% (Sigma Aldrich) and with a 5% of dodecyl benzene sulfonic acid (DBSA) surfactant (Sigma Aldrich), in order to enhance its electrical conductivity.[27,28] The transistor channels of 1 mm width have been patterned on a glass slide of 2.5 × 7.5 cm and the PEDOT:PSS has been spun onto the substrate at 1500 RPM for 30 s. The film thickness is $d \sim 80$ nm. Slides were finally baked on a hot plate at 120 °C for 75 min. A PDMS well of about 100 μL volume has been used to confine the electrolyte solution upon the channel of the transistor, the channel defined by the overlapping of the electrolyte with the organic polymer. The final device aspect ratio is $L/W = 10$ (channel width $W = 1$ mm, channel length $L = 10$ mm). Electrical measurements with the OECT device were obtained by a 2 channel source/measure precision unit (Agilent B2902A), controlled by a home-made LabView software.

2.2 Synthetic eumelanin

Synthetic eumelanin was prepared by oxidative polymerization of 5,6-dihydroxyindole (DHI) with the horseradish peroxidase/hydrogen peroxide system, as described previously.[29] Eumelanin concentration in aqueous suspensions is defined in terms of formal monomer concentration (DHI, M_w 149).

3 Results and discussions

3.1 The device

Fig. 1 shows a schematic view of the OECT electrical circuit and the sensing mechanism in the case of eumelanin biopolymer dispersed at several concentrations in Phosphate Buffered Saline (PBS) solution. The device active layer is made of PEDOT:PSS, a conductive polymer with excellent biocompatibility properties.[15,22,23] The gate electrode, aimed at inducing an electrochemical reaction in the presence of eumelanin, consists of a platinum wire, while source and drain electrodes are made of silver.

Fig. 2a shows the output characteristics (I_{ds} *vs.* V_{ds}, at different gate voltages, V_{gs}) of the device measured in PBS 0.1 M with eumelanin at 10^{-9} M formal concentration suspended in solution. The transfer characteristics (expressed as current modulation $\Delta I_{ds}/I_{ds,0}$ *vs.* V_{gs}, $V_{ds} = -0.4$ V) are shown in Fig. 2b for the highest concentration of eumelanin (10^{-2} M) and for the PBS electrolyte solution based device, acting as a blank.

Output curves were acquired by sweeping V_{ds} between 0 and −0.8 V, in steps of 0.1 V, at fixed V_{gs} between 0 and 0.8 V (V_{gs} steps of 0.1 V). Transfer characteristics of OECT were acquired by measuring I_{ds} *vs.* time, fixing V_{ds} at −0.4 V and

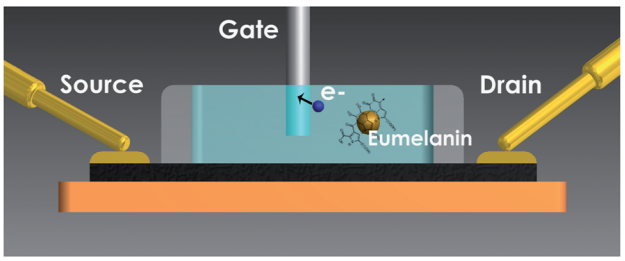

Fig. 1 Schematic diagram and electrical circuit of the OECT-based biosensor for the detection of eumelanin pigment in colloidal suspension, here a saline electrolyte solution (PBS 0.1 M). The black stripe represents the active layer of PEDOT:PSS, the OECT channel being defined by the overlapping of the electrolyte with the polymer. The figure also represents the mechanism for the pigment detection, based on a redox reaction of eumelanin at the gate electrode.

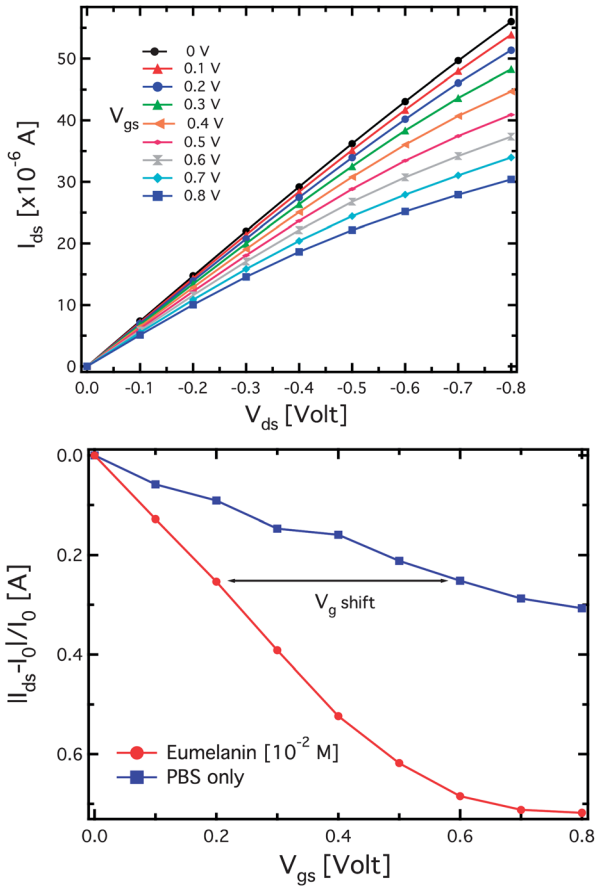

Fig. 2 (a) Output characteristics of the OECT measured with eumelanin at the concentration of 10^{-9} M suspended in 0.1 M PBS. (b) Transfer characteristics of the OECT with a Pt gate electrode characterized both with eumelanin in suspension and without (0.1 M PBS only), $V_{ds} = -0.4$ V.

pulsing V_{gs} between 0 V and 0.8 V with a step of 0.2 V. The source–gate current (I_{gs}) was acquired simultaneously during I_{ds} measurement in order to monitor the electron transfer reaction occurring at the gate electrode. The I_{gs} acquisition provides information both on the operational mode of the OECT, that is faradaic or non-faradaic mode,[21] and on the electrical and redox activity of the eumelanin components. It is assumed that catechol-type structures belonging to reduced DHI units undergo oxidation at the gate electrode providing electrons to the I_{gs} current of the gate circuit. For each V_{gs} step applied across the gate electrolyte, the drain current was acquired for 60 s, *e.g.* a long time scale aimed at achieving a nearly steady drain current value for the related V_g, shown by a saturation of the channel current in time. The phosphate buffer solution (PBS) (pH = 7.2) was used as the electrolyte for all the measurements to ensure pH stabilization. The application of V_{ds} induces a drift of the holes along the PEDOT:PSS channel, generating a drain–source current (I_{ds}). Upon application of a positive gate voltage (V_{gs}), cations (M^+) from the electrolyte enter the PEDOT:PSS channel causing its de-doping according to the eqn (1):[30]

$$PEDOT^+{:}PSS^- + M^+ + e^- \leftrightarrow PEDOT^0 + M^+{:}PSS^- \quad (1)$$

This is referred to as the de-doping process, as its effect causes a decrease in the modulus of drain current $|I_{ds}|$.[31] This effect is due to the smaller number of holes available for conduction, as a consequence of incorporation of cations into the PEDOT:PSS backbone. Here, according to eqn (1), cations tend to be adsorbed by the $PEDOT^+{:}PSS^-$ thin film causing a reduction of the oxidized $PEDOT^+$ and a consequent decrease of conductivity upon reduction to the reduced form $PEDOT^0$. This process is reversible, in fact, when V_{gs} is switched off ($V_{gs} = 0$ V), ion diffusion occurs from the PEDOT:PSS to the electrolyte, increasing the number of conducting holes and, consequently, $|I_{ds}|$. Such a process is referred to as doping.[17] In this paper, the OECT current response is expressed as current modulation $\Delta I/I_0 = (I - I_0)/I_0$, where I is the drain current value measured for $V_{gs} > 0$ V and I_0 is the I_{ds} value for $V_{gs} = 0$ V.[17,21] The current values were determined from current transient measurements considering the quasi-steady state current level.

3.2 Eumelanin response in the OECT device

Eumelanin sensing is based on the redox behaviour of the polymer in contact with the gate electrode. In detail, oxidation of eumelanin units at the Pt gate electrode–electrolyte interface promotes electron injection into the gate electrical circuit. As a consequence, the OECT is said to work under a faradaic regime, characterized by a negligible potential dropping at the gate–electrolyte interface.[17,32] In this operating regime the applied gate voltage is almost entirely transferred as effective gate voltage (V_g^{eff}) acting at the electrolyte–polymer interface and the cations produced upon DHI oxidation in the electrolyte are forced to move toward the PEDOT:PSS by the gate voltage. The sensing mechanism would therefore be similar to the sensing of hydrogen peroxide,[32] halide,[21] or dopamine[33] previously reported with OECT devices operating in faradaic mode.[17] However, in all the above cases the sensing process was aimed at monitoring soluble components, and the electrical behaviour of insoluble polymer suspensions has been so far little explored.[2] Fig. 3a shows the OECT response ($\Delta I/I_0$) as a function of the eumelanin concentration for two gate voltages ($V_g = 0.3$ V and $V_g = 0.6$ V). The dynamic sensing range spans between 1×10^{-6} M and 1×10^{-2} M, the signal becoming about 3-times larger for $V_g = 0.6$ V and reaching a modulation value close to 0.8 for the highest concentration of 10^{-2} M.

In detail, above 1.3×10^{-6} M the OECT response increases almost monotonically from a value of about 0.25 up to 0.79, indicating an increase of 0.54 in current modulation, corresponding to an increase of about 86% with respect to the base signal. In Fig. 2b, showing the transfer curves of OECT characterized both without and with eumelanin suspension, the transfer curve shifts to a lower gate voltage (hundreds of mV), indicating that the effective gate voltage (V_g^{eff}) is increased due to the electro-oxidation of eumelanin at the Pt gate electrode. Fig. 3b shows the expected gate current increase in the presence of eumelanin, such an increase being the fingerprint of the faradic mode of operation.[21,34]

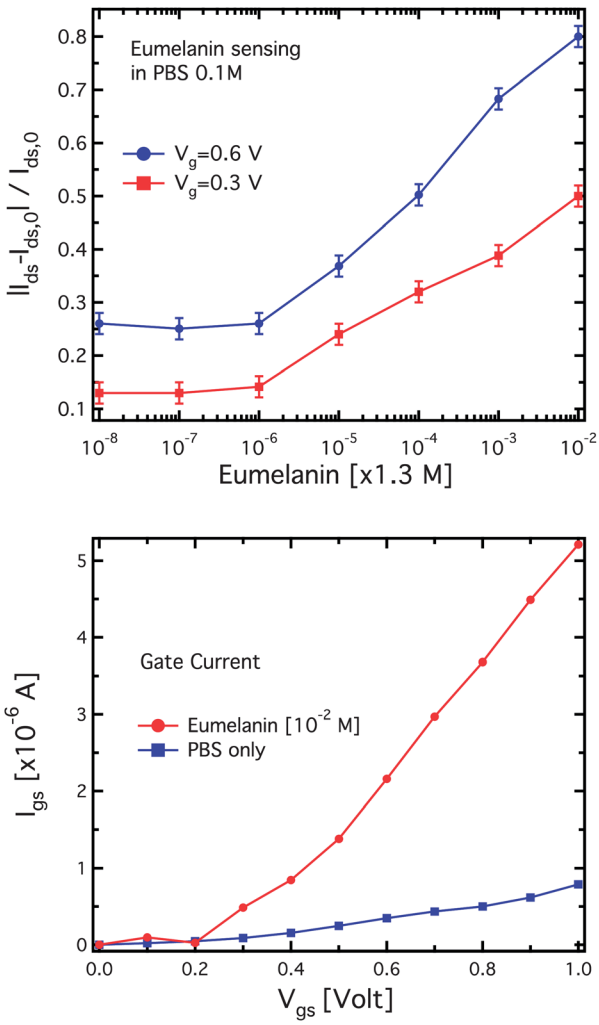

Fig. 3 (a) Sensing plot ($\Delta I/I_0$ *vs.* concentration) expressed as the OECT response at varying eumelanin concentrations, for an OECT sensor working with a Pt gate electrode. (b) Corresponding OECT gate current flowing in the gate circuit, with (red curve) and without (blue curve, PBS electrolyte only) the eumelanin in suspension; when the pigment is not present in solution, no faradaic gate current is flowing and the OECT is working under a capacitive (non-faradaic) mode of operation.

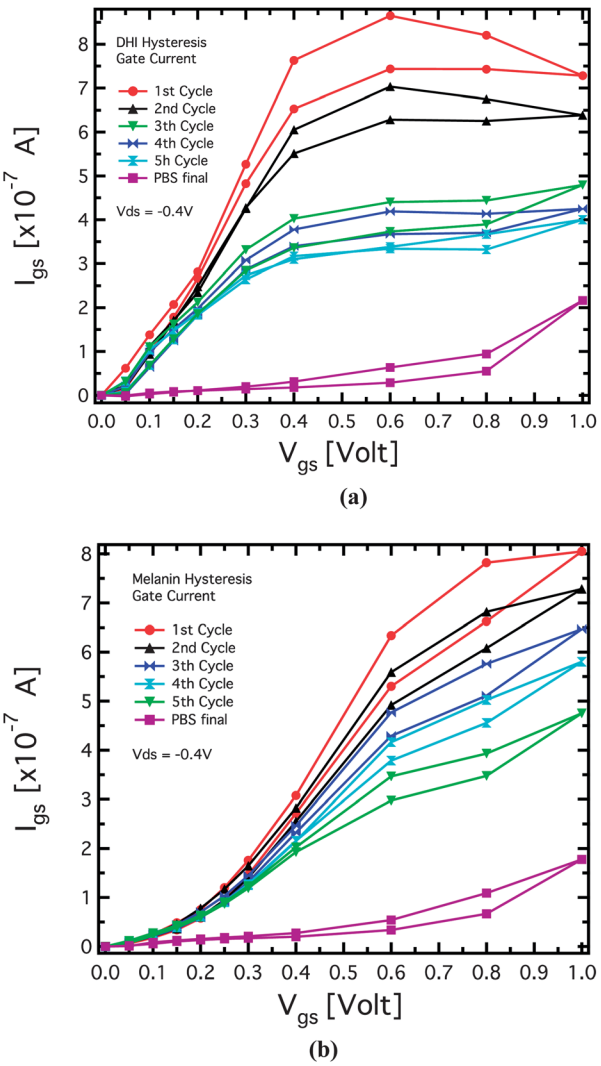

Fig. 4 Hysteresis loop cycles of the gate current acquired for DHI (a) and eumelanin pigment (b). $V_{ds} = -0.4$ V.

3.3 Eumelanin *versus* DHI redox behaviour

A close analysis of device curves in the presence of eumelanin or DHI gave some qualitative insight into the effect of the ionic circuit (gate–source current, I_{gs}) on the underlying electronic circuit (drain–source current, I_{ds}). An initial consideration regards the PBS-based benchmark device. In the latter, the leakage through the gate related to the PBS solution provides the baseline for comparing eumelanin and DHI, since both the gate current value (much lower than those exhibited by eumelanin and DHI) and the small hysteresis are preserved in different testing devices, denoting an excellent reproducibility. On this basis, analysis of OECT features may allow for a reliable comparison between the electrical properties of eumelanin and DHI.

Data in Fig. 4a and b, obtained by recording cyclically (5 cycles) hysteretic I_{gs} loops in the presence of eumelanin- and DHI-based electrolytes, allowed for an insightful analysis of the ionic circuit. The data acquisition mode (*i.e.*, long time scale between adjacent step voltages for the saturation of the polymer dedoping process) would ensure control of the hysteresis shape and minimization of memory effects[35] and/or trapping/detrapping phenomena. Since a PBS based device does not display a faradaic behaviour in the presence of a Pt gate electrode, the observation that the initial gate current in the DHI- and eumelanin-based testing devices is almost 5 times higher than that recorded for the benchmark system would clearly provide a demonstration for the faradaic behaviour induced by the biopolymer and the indole monomer. Interestingly, the curves in Fig. 4a and b show that both the gate current and the area subtended by each loop gradually decrease following each cycle, the latter approaching baseline behaviour.

Hysteresis is known to reflect the mismatch between the scan rate and the time scale on which doping/dedoping occurs. On this basis, the hysteretic behaviour of eumelanin- and DHI-based devices would suggest a progressive and irreversible alteration of the samples associated with a decreased redox

activity for both polymer and monomer following repeated modification of their redox states.[36] Consistent with this interpretation, a partial or complete loss of response was observed in the case of eumelanin samples that were allowed to stand for prolonged periods of time as suspensions without deoxygenation or deep freezing.

The analysis of the shapes of the I_{gs} curves shows in the case of DHI a saturating behaviour starting at $V_g = 0.6$ V of gate bias, which was not apparent in the eumelanin-based devices, where a monotonic trend was visible in the spun gate voltage range. This behaviour could indicate that the redox activity of DHI is almost saturated at lower voltages compared to the eumelanin, in accord with a substantial conversion to less responsive polymeric components during the initial cycles. Generally, as mentioned above, a gate voltage shift is expected for faradaic like systems due to redox transformation of the analytes at the gate electrode, resulting thus in an effective gate bias drop at the dielectric–polymer interface. As a consequence, a more efficient ionic penetration inside the polymeric layer is induced and a stronger channel current modulation occurs at lower gate biases. This is apparent from the shift toward lower gate voltage biases of transfer curves recorded in the presence of DHI or eumelanin relative to the PBS baseline prototype (see Fig. 2b). Another important implication of the effective gate voltage can be shown by coupling the Bernard's equation of OECT source–drain current (1a) and the expression of the effective gate voltage[31] (1b):

$$I_{ds} = -\frac{G(V_g - V_p)^2}{2V_p} \quad (1a)$$

$$V_g^{eff} = V_g + (1+\gamma)\frac{kT}{2e}\ln[M] + \text{const.}, \quad (1b)$$

where G is the conductance of the organic semiconductor, V_p is the pinch-off voltage, γ is the ratio between the capacitances of the two interfaces (electrolyte–PEDOT:PSS and electrolyte–gate),[32] k is the Boltzmann's constant, T is the absolute temperature and e is the elementary charge. As a result, a linear dependence of the source–drain current on the logarithm of the concentration is predicted:

$$I_{ds} \sim \frac{G}{V_p}\frac{KT}{2e}\ln[M] + \cos t(V_g, V_p) \quad (2)$$

This linear relationship between I_{ds} and ln[M] was experimentally confirmed, as shown in Fig. 3a, where the curves of the OECT response as a function of ln[M] are nearly linear in the dynamic range investigated (that is from 10^{-6} M up to 10^{-2} M).

3.4 Real-time monitoring

In order to study the drain current evolution at fixed voltages, I_{ds} was monitored upon *in situ* addition of eumelanin. The OECT response was monitored in real-time ($V_{gs} = 0.6$ V, $V_{ds} = -0.4$ V) following injection of 10 μL eumelanin suspension during acquisition. Fig. 5 shows that in real-time mode the OECT sensor is eumelanin-sensitive down to the nM range, the sensor reacting almost instantaneously with a rapid relative change of the drain current ($\Delta I_{ds} \sim 1$ μA) in less than 3 s. A more significant $|I_{ds}|$ decrease was observed at higher concentrations (10^{-8} to 10^{-7} M). Since the sensitivity of the OECT device is higher in the real-time monitoring mode compared to the dynamic range achieved by the modulation response, as previously observed with other bioanalytes,[33,37] it can be concluded that 10^{-9} M is the lowest detection limit for the eumelanin pigment in the OECT.

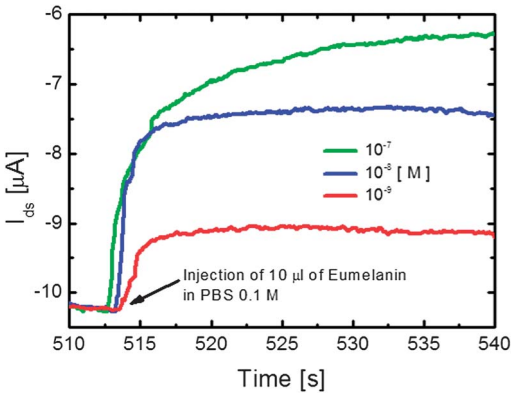

Fig. 5 Drain–source current *vs.* time of the OECT characterized upon addition of a 10 μL drop of eumelanin at different concentrations. It is found that the lowest eumelanin detection limit of OECT in real-time mode is 1×10^{-9} M. The black arrow represents the exact time of injection of the drop.

3.5 Toward a chemical model for eumelanin electrical response

Eumelanin formation from DHI is known to involve oxidative polymerization of indole *via* the 2-, 4- and 7-positions of the indole ring to give mixtures of oligomeric/polymeric chains at various levels of oxidation (Scheme 1). Depending on the reaction conditions, the redox characteristics of the environment and the extent of polymer exposure to oxygen and other oxidizing agents (*i.e.* the extent of "aging"), the relative proportion of reduced (catechol, DHI) *versus* oxidized (indolequinone) units may vary significantly.

Both the key features of the curves in Fig. 4b, *i.e.* the progressive decrease in gate current and hysteretic loop areas, would suggest that in fresh eumelanin samples the catechol–quinone units are initially "frozen" by the mode of aggregation of the molecular components into a redox state that is far from the equilibrium and that the repeated redox interaction with the gate electrode provides the input for a progressive redistribution of the redox centres within the polymer, leading eventually to a more stable, overall less responsive electronic arrangement. In line with this view, the low or null response of "aged" eumelanin samples might suggest either a higher degree of oxidation of indole units or the slow spontaneous attainment of the final equilibrium conditions between the interacting redox centres of the polymer aggregates.

On the other hand, the analogous behaviour of DHI in solution may be interpreted by assuming that the initial oxidation product, 5,6-indolequinone, as soon as it is generated, is immediately trapped by the excess reduced indole

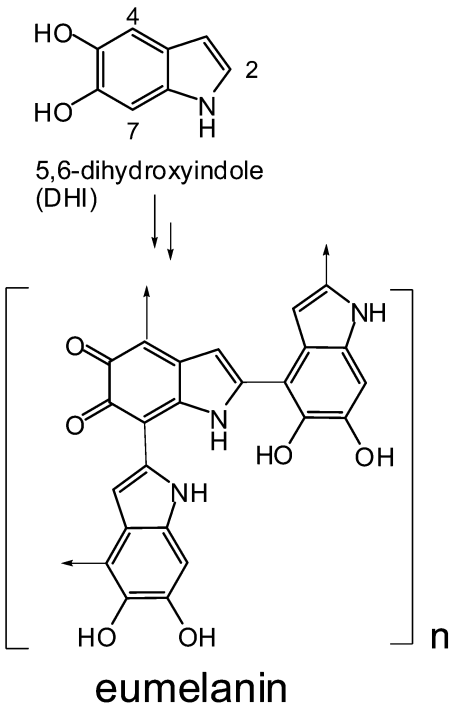

Scheme 1 Simplified view of eumelanin formation by oxidative polymerization of DHI. A representative structural motif is highlighted, showing the coexistence in the polymer of oxidized (quinone) and reduced (catechol) units.

present in solution to give eumelanin-like intermediates that irreversibly alter the analyte electric response after each cycle.

Since injection of electrons from the eumelanin into the gate electrode can occur only from reduced DHI units (Scheme 2), the voltage values determined by the OECT device may be taken as roughly reflecting the proportion of reduced indole units in the polymer. It is noted that DHI unit oxidation results in the generation of protons in the medium, which may be involved in the ionic circuit.

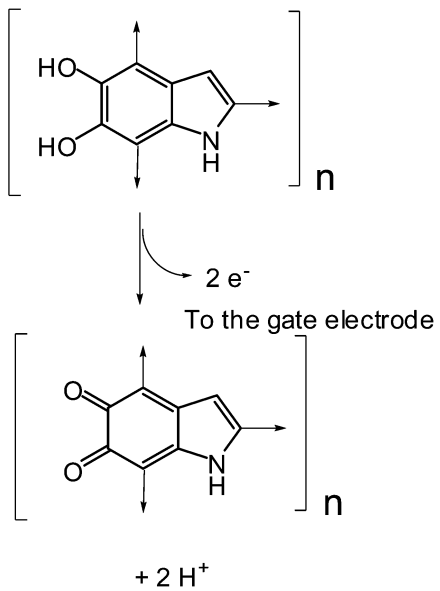

Scheme 2 Schematic illustration of eumelanin oxidation at the gate electrode. Reduced DHI units release two electrons and two protons to generate oxidized quinone units.

An interesting implication is that, taking the OECT response of monomer DHI in solution as the maximum response of a hypothetical, fully reduced eumelanin sample, with the null response of an oxidized (aged) eumelanin sample at the opposite extreme, it could be possible in principle to gain information about the average redox state of a given polymer sample simply by determining its onset voltage relative to that of DHI. From the data in Fig. 3, for example, it can be concluded that the oxidation potential of the investigated eumelanin samples approaches a value that is around 200 mV, suggesting a similar proportion of reduced catechol units. This is a rough estimation and a more accurate evaluation requires the application of narrower gate bias steps below 200 mV. It would be interesting to compare these data with those obtained in a previous study on the electrochemical behaviour of DHI polymer films,[14] which gave an oxidation potential $E_{1/2}$ of 150 mV. Therefore our interpretation of the threshold oxidation potential could be reasonable.

4 Conclusion

In this paper we report for the first time the characterization of the electrical properties of an insoluble eumelanin sample as an aqueous suspension using OECT technology. The most outstanding finding of this study that deserves further investigation is the high sensitivity of the device response to eumelanin, supporting a hitherto unrecognized versatility of the OECT for sensing insoluble redox active materials. In this respect, gate current analysis underscored the ability of the dynamic DHI–quinone system in the fresh eumelanin biopolymers to exchange electrons with the gate even under heterogeneous phase conditions by shuttling between accessible redox states. Worthy of note is also the observed abatement in current intensity with decreased hysteretic loop area after each cycle suggesting irreversible conversion of eumelanin from an originally unstable electronic arrangement toward a π-equilibrated state less responsive to the gate electrode. Elucidation of the processes underlying gate current characteristics and hysteretic behaviour of eumelanin may not only guide ongoing efforts toward the rational design and implementation of bio-inspired devices with tailored electrical behaviour for bio-electronics, but may yield new insights into the redox properties of the biopolymer that have otherwise escaped previous investigations.

Acknowledgements

This research is supported by the project BioNiMed (Multifunctional Hybrid Nanosystems for Biomedical Applications) from Fondazione Cassa di Risparmio di Parma (CARIPARMA) and by the N-Chem project within the CNR–NANOMAX Flagship program. This work was also supported by the Italian Ministry of Research and Education (MIUR) with a grant to MdI (PRIN 2010-2011-010PFLRJR project), and was carried out in the frame

of the EuMelaNet program (http://www.espcr.org/eumelanet/). Authors acknowledge Marco Pola for technical assistance and Vibo Srl (Milan) for technical support. We gratefully acknowledge Fabio Cicoira and Clara Santato for fruitful discussions.

References

1 M. d'Ischia, A. Napolitano, A. Pezzella, P. Meredith and T. Sarna, *Angew. Chem., Int. Ed.*, 2009, **48**, 3914–3921.
2 P. Meredith and T. Sarna, *Pigm. Cell Res.*, 2006, **19**, 572–594.
3 J. D. Simon, D. Peles, K. Wakamatsu and S. Ito, *Pigm. Cell Melanoma Res.*, 2009, **22**, 563–579.
4 G. Prota, M. d'Ischia and D. Mascagna, *Melanoma Res.*, 1994, **4**, 351–358.
5 J. D. Simon, L. Hong and D. N. Peles, *J. Phys. Chem. B*, 2008, **112**, 13201–13217.
6 M. Ambrico, P. F. Ambrico, A. Cardone, N. F. Della Vecchia, T. Ligonzo, S. R. Cicco, M. M. Talamo, A. Napolitano, V. Augelli, G. M. Farinola and M. d'Ischia, *J. Mater. Chem. C*, 2013, **1**, 1018–1028.
7 M. D'Ischia and G. Prota, *Pigm. Cell Res.*, 1997, **10**, 370–376.
8 L. Zecca, F. A. Zucca, H. Wilms and D. Sulzer, *Trends Neurosci.*, 2003, **26**, 578–580.
9 H. Lee, S. M. Dellatore, W. M. Miller and P. B. Messersmith, *Science*, 2007, **318**, 426–430.
10 N. F. Della Vecchia, R. Avolio, M. Alfè, M. E. Errico, A. Napolitano and M. d'Ischia, *Adv. Funct. Mater.*, 2013, **23**, 1331–1340.
11 J. McGinness, P. Corry and P. Proctor, *Science*, 1974, **183**, 853–855.
12 P. Meredith, C. J. Bettinger, M. Irimia-Vladu, A. B. Mostert and P. E. Schwenn, *Rep. Prog. Phys.*, 2013, **76**, 034501.
13 A. Mostert, B. J. Powell, F. L. Pratt, G. R. Hanson, T. Sarna, I. R. Gentle and P. Meredith, *Proc. Natl. Acad. Sci. U. S. A.*, 2012, **109**, 8943–8947.
14 S. Gidanian and P. J. Farmer, *J. Inorg. Biochem.*, 2002, **89**, 54–60.
15 A. Richter-Dahlfors, K. Svennersten, K. C. Larsson and M. Berggren, *Biochim. Biophys. Acta, Gen. Subj.*, 2011, **1810**, 276–285.
16 G. Tarabella, F. Mahvash Mohammadi, N. Coppede, F. Barbero, S. Iannotta, C. Santato and F. Cicoira, *Chem. Sci.*, 2013, **4**, 1395–1409.
17 F. Cicoira, M. Sessolo, O. Yaghmazadeh, J. A. DeFranco, S. Y. Yang and G. G. Malliaras, *Adv. Mater.*, 2010, **22**, 1012–1016.
18 P. N. Bartlett, P. R. Birkin, J. H. Wang, F. Palmisano and G. De Benedetto, *Anal. Chem.*, 1998, **70**, 3685–3694.
19 S. Y. Yang, F. Cicoira, R. Byrne, F. Benito-Lopez, D. Diamond, R. M. Owens and G. G. Malliaras, *Chem. Commun.*, 2010, **46**, 7972–7974.
20 Z. T. Zhu, J. T. Mabeck, C. Zhu, N. C. Cady, C. A. Batt and G. G. Malliaras, *Chem. Commun.*, 2004, 1556–1557.
21 G. Tarabella, C. Santato, S. Y. Yang, S. Iannotta, G. G. Malliaras and F. Cicoira, *Appl. Phys. Lett.*, 2010, **97**, 123304.
22 P. Lin, F. Yan, J. Yu, H. L. W. Chan and M. Yang, *Adv. Mater.*, 2010, **22**, 3655–3660.
23 J. Isaksson, P. Kjall, D. Nilsson, N. D. Robinson, M. Berggren and A. Richter-Dahlfors, *Nat. Mater.*, 2007, **6**, 673–679.
24 D. Khodagholy, T. Doublet, M. Gurfinkel, P. Quilichini, E. Ismailova, P. Leleux, T. Herve, S. Sanaur, C. Bernard and G. G. Malliaras, *Adv. Mater.*, 2011, **23**, H268–H272.
25 S. Y. Yang, B. N. Kim, A. A. Zakhidov, P. G. Taylor, J.-K. Lee, C. K. Ober, M. Lindau and G. G. Malliaras, *Adv. Mater.*, 2011, **23**, H184–H188.
26 A. Richter-Dahlfors, D. T. Simon, S. Kurup, K. C. Larsson, R. Hori, K. Tybrandt, M. Goiny, E. H. Jager, M. Berggren and B. Canlon, *Nat. Mater.*, 2009, **8**, 742–746.
27 J. Ouyang, Q. Xu, C.-W. Chu, Y. Yang, G. Li and J. Shinar, *Polymer*, 2004, **45**, 8443–8450.
28 X. Crispin, S. Marciniak, W. Osikowicz, G. Zotti, A. W. D. van der Gon, F. Louwet, M. Fahlman, L. Groenendaal, F. De Schryver and W. R. Salaneck, *J. Polym. Sci., Part B: Polym. Phys.*, 2003, **41**, 2561–2583.
29 L. Ascione, A. Pezzella, V. Ambrogi, C. Carfagna and M. d'Ischia, *Photochem. Photobiol.*, 2013, **89**, 314–318.
30 D. Nilsson, N. Robinson, M. Berggren and R. Forchheimer, *Adv. Mater.*, 2005, **17**, 353.
31 D. A. Bernards and G. G. Malliaras, *Adv. Funct. Mater.*, 2007, **17**, 3538–3544.
32 D. A. Bernards, D. J. Macaya, M. Nikolou, J. A. DeFranco, S. Takamatsu and G. G. Malliaras, *J. Mater. Chem.*, 2008, **18**, 116–120.
33 H. Tang, P. Lin, H. L. W. Chan and F. Yan, *Biosens. Bioelectron.*, 2011, **26**, 4559–4563.
34 F. Lin and M. C. Lonergan, *Appl. Phys. Lett.*, 2006, **88**, 133507.
35 M. C. Lonergan, C. H. Cheng, B. L. Langsdorf and X. Zhou, *J. Am. Chem. Soc.*, 2002, **124**, 690–701.
36 R. Edge, M. D'Ischia, E. J. Land, A. Napolitano, S. Navaratnam, L. Panzella, A. Pezzella, C. A. Ramsden and P. A. Riley, *Pigm. Cell Res.*, 2006, **19**, 443–450.
37 G. Tarabella, A. G. Balducci, N. Coppedè, S. Marasso, P. D'Angelo, S. Barbieri, M. Cocuzza, P. Colombo, F. Sonvico, R. Mosca and S. Iannotta, *Biochim. Biophys. Acta, Gen. Subj.*, 2013, **1830**(9), 4374–4380.